

# A NUMERICAL INVESTIGATION OF TURBULENT FLOW IN CIRCULAR U-BEND

A. Miloud<sup>1</sup>, M. Aounallah<sup>1</sup>, O.Imine<sup>2</sup> and M. Guen<sup>1</sup>  
University of Science and Technology of Oran Mohamed Boudiaf (USTO-MB)  
Department of Maritime Engineering  
<sup>1</sup>Laboratory Aero-Hydrodynamic Naval  
<sup>2</sup>Laboratory Aeronautic and Propulsion Systems  
B.P 1505 El M'naouer Oran-Algeria

## Abstract

Numerical investigations of turbulent flows through a circular 180° curved bend with defined as the bend mean radius to pipe diameter for a Reynolds number of  $4.45 \times 10^4$  is presented in this study . The computation domain is performed for a U-Bend with full long pipes at the entrance and at the exit. Two turbulence models were tested in this work. The commercial software ANSYS FLUENT is used to solve the steady Reynolds–Averaged Navier–Stokes (RANS) equations. The numerical results were compared with experimental data for presenting their capabilities to capture the formation and extend this turbulence driven vortex. The results of numerical simulations of turbulent flow 3D heat transfer are presented for the case of two channels U turn and rectangular.

The purpose of this investigation was to study the effect of the corrugated walls of the heated portion on the improvement of cooling, in particular the influence of the wave length. The calculations were performed for a Reynolds number of 10,000 set at two values of the number of rotation ( $Ro = 0.0$  to  $0.14$ ) and a report of limited density to  $0.13$ . In these simulations, ANSYS FLUENT code was used to solve the Reynolds equations expressing the relations between the different fields' averaged variables over time. Model performance k-omega SST and model RSM are evaluated through a comparison of the numerical results obtained for each model and the experimental and numerical data. In this thesis, detailed average temperature predictions, the scope of the secondary flow and distributions of the local Nusselt are presented. It turns out that the corrugated configuration further urges the heat exchange provided to reduce the velocity of the coolant within the channel.

**Keywords:** cooling blades - corrugated walls – models k-omega SST and RSM- Fluent code- rotation effect

## 1 Introduction

Gas turbine performance and particularly their thermal efficiency have continued to suffer dramatic progress since the Second World War. In aeronautics, military applications have seen increasing power / weight ratio, while in civil aviation, fuel consumption has dropped significantly. The technology in the field of turbomachinery is also important in energy production systems, so that the performance of the turbines duality/blade cooling efficiency is needed in the same way as in aeronautics.

The improved performance and yields of jet engines means increasing the temperature of the gas in the combustion chamber. Temperatures imposed turbines are very high and adverse thermal effects resulting pushing manufacturers continually improve cooling techniques thermally stressed parts, such as: combustion chambers, the blades distributors of high and low pressure turbines, blades of high and low pressure turbines, pressurization bearing compressors and turbines, accessories, fairings and radial arms, as problems to solve imposed these processes.

It is clear that to increase the efficiency of gas turbines, it is essential to increase the turbine inlet temperature. Nowadays, the inlet temperatures of the gas turbine blades can reach 1700 ° C and the materials used in this case are only able to withstand 1200 ° C A1300 ° C. The cooling air extracted from the compressor is of the order of 650° C, it can be passed through small channels drilled inside the blades and lowering the temperature to about 1000 °C, which is reasonable for a reliable operation of the turbojet.

The curvature of the blade and the rotation simultaneously affect the stability of the boundary layer. A convex surface prevents the generation of turbulence, while a concave surface increases the generation of turbulent energy. The consequence is that the heat transfer increases in the concave portion (base) and decreases in the convex portion (surface), and when one combines the increase in temperature in highly non-uniform character of the thermal field, it becomes essential to adopt a carefully optimized cooling process in order to ensure as uniform temperature distribution as possible so that the overall efficiency no less impaired.

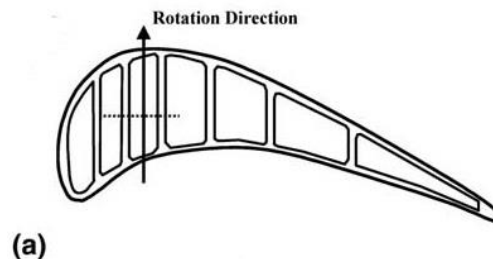
The adoption of a cooling process is essential if one wants to keep an acceptable lifetime of the turbine, since it is directly related to the heat load. In fact, cooling of the contact surfaces allows the hot gases to increase the maximum temperature of the cycle while keeping the surface temperature within acceptable limits.

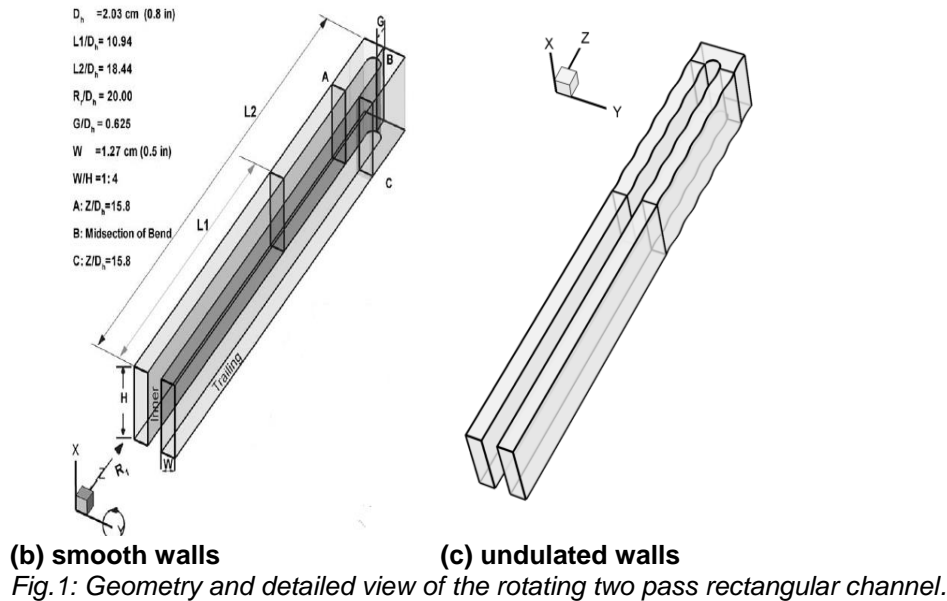
## 2 Problem Position

Figure 1 shows the duct tested with an aspect ratio:  $AR = 1:4$  with the definition of geometrical parameters. Except the wavy form the heated part, the same geometrical features of the rectangular channel treated by Guoguang et al. (3) is considered in the present study. The total length of the channel,  $L$ , equals to 37.47cm, divided on an unheated smooth starting section ( $L_1 = 22.23$  cm) and a heated wavy section ( $L_2 = 15.24$  cm). The channel width  $W$  is kept the same at 1.27 cm and the channel height  $H$  is fixed to 5.08 cm to get an aspect ratio  $AR = W/H = 1:4$ . The number of the undulation and its amplitude on the wavy part is taken 10 and  $0.05 W$  respectively. The distance from the inlet of the channel to the axis of rotation is given by  $R_r = 40.64$  cm. The radius of curvature of the 180° sharp turn is  $r_i = 0.635$  cm) and the minimum gap  $G$  between the inner and outer surfaces of the bend is 1.27cm. The two side walls facing the rotational direction are denoted as leading and trailing surfaces, while the other two are denoted as inner and outer surfaces. To show the effect of the wavy heated surfaces on the global heat transfer and the temperature of the air at the exit, a new configuration is produced different by the undulated shape of their heated surfaces and keeping the same dimensions of the overall parts. The mean Nusselt number decreases in comparison to the square cavity with smooth walls. The undulation equation is expressed as follows:

$$f(y) = [1 - b + b(\cos 2 \pi n y)] \quad (1)$$

Where  $n$  and  $b$ , are respectively the number of undulations and the amplitude.





### 3 Computation Procedure

The viscous incompressible turbulent flow is described by Navier-Stokes equations completed by the energy equation and one of the two turbulence models: the shear stress  $K\omega$  SST and the Reynolds stress model RSM. The latter model is based on the linear pressure-strain and wall treatment is modelled with standard wall function. The governing equations were described in detail in the literature. Since the Mach number is quite low, the flow is considered to be incompressible. However, the density in the centrifugal force terms is approximated by  $\rho = \rho_0 T_0/T$  to account for the density variations caused by the temperature differences.

Where  $\rho_0$  and  $T_0$  are the density and temperature at the inlet of the cooling channel. The density variation caused by the pressure gradients induced by the channel rotation is neglected since the corresponding experiment condition gives a maximum density variation of only about 1.1% from the inlet to the exit of the duct at the highest rotation number. So it is realistic to neglect the density variation caused by the pressure gradients induced by the channel rotation. A constant velocity is fixed at the inlet of the duct ( $Z = 0$ ). The coolant air became fully developed turbulent velocity profile before entering the heated section since the unheated length ( $L1$ ) is sufficient long. At the exit of the duct, zero-gradient boundary conditions were specified for the mean velocity and all turbulent quantities. The coolant fluid at the inlet of the rectangular channel is air at uniform temperature:

$$T = T_0 \text{ (i.e., } \theta = (T - T_0)/(T_w - T_0) = 0) \quad (2)$$

The wall temperature of the unheated sections is kept constant at  $T = T_0$  ( $\theta = 0$ ) while the wall temperature of the heated section is kept constant at  $T = T_w$  ( $\theta = 1$ ).

All the simulations are done with the commercial code: ANSYS Fluent 6.3.26 which uses the finite volume method to discretized the partial differential equations on a grid where all the variables are collocated with a segregated implicit solver based on the pressure. The second order upwind scheme is employed for the convection term in the momentum, energy and turbulence equations. The pressure-velocity coupling is ensured using the SIMPLE algorithm. The residuals of continuity, momentum and energy equations are required to be below  $10^{-5}$  in order to reach a fully converged solution.

### 4 Grid Generation

The computational domain is filled with a non-uniform rectangular grid with a very fine spacing near the walls, as needed for accurately resolving the steep gradients in the thin buoyancy driven boundary layer. The geometry and the grid are generated using Gambit preprocessor taking into account the boundary layer refinement. Figure 2 shows the coarse grid for the undulated rectangular duct with

AR = 1:4 meshed into 514 560 hexahedral control volumes. The height of the first cell is calculated through the estimating value of  $y^+$  which guaranteed the using of the low Reynolds number turbulence models. It is also desirable to obtain an asymptotically grid-independent solution by means of refined grid.

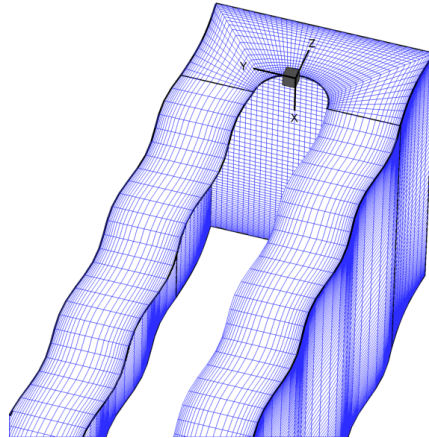


Fig. 2: The hexahedral coarse grid of the undulated rectangular channel.

To determine the accuracy of the numerical solution, the grid-independent study using both turbulence models on three grids: 514 560, 1 165 056 and 1 916 928 hexahedral cells. Table 1 shows the temperature of the air at the exit for  $Re = 10\,000$ , two rotation number ( $R_0 = 0.0$ ,  $R_0 = 0.14$ ) and coolant-to-wall density ratio  $(1 - (T_0 / T_w)) = 0.13$  for the smooth channel and the wavy one. As it can be seen, slight difference of the air temperature at the exit of the rectangular channel is observed between the medium and the fine grids. Since no appreciable difference exists between the solutions of the grids tested, the grid of 1 165 056 is retained for all subsequent calculations.

Geom.	$R_0$	Models	Coarse	Medium	Fine
Smooth channel	0.0	SST	313.80	314.55	314.22
		RSM	317.37	320.95	321.27
	0.14	SST	314.65	314.25	314.19
		RSM	318.50	316.80	316.15
Wavy channel	0.0	SST	314.90	314.50	314.81
		RSM	320.04	321.46	320.34
	0.14	SST	315.18	315.10	314.50
		RSM	321.03	319.20	318.86

Table 1. Outlet temperature predictions comparison between the smooth and undulated rectangular channel ( $Re = 10\,000$ ,  $\Delta\rho / \rho = 0.13$ ) for different grids.

Fig. 3 shows the wall  $y^+$  distribution in particularly on the heated part of the channel obtained by the  $k-\omega$  SST model. This figure shows the whole of the domain having a moderate value of  $y^+ \approx 5$  to 7 confirming that the resolution used agree satisfactory with the turbulence model type. The numerical results predict a slight large value of the  $y^+$  in the inner side of the curved part due certainly to the acceleration of the fluid flow in this region.

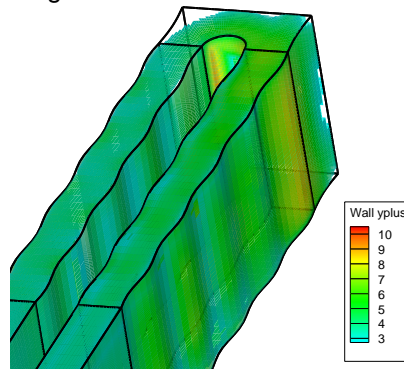


Fig. 3. : Wall  $y^+$  distribution on the heated part of the channel predicted by  $k-\omega$  SST model.

## 5 Results and Discussion

This section presents the three-dimensional mean flow, the temperature field and the Nusselt number ratios for the smooth and the undulated ducts tested. Fig. 4 shows the dimensionless temperature contour  $\theta$  and the velocity vector field in the heated section at the middle plane between the leading and trailing surfaces for a Reynolds number of  $Re = 10\,000$ , a rotation number  $R_0 = 0.14$  and coolant-to-wall density ratio  $\Delta\rho/\rho = 0.13$ . It is clearly seen that the area of the cold air decreases going to the 180° sharp turn and still concentrate in the center of the first passage. The heat transfer characteristic is significantly different in the second pass by the presence of the secondary flows induced by the bend. At the corners of the bend, thin thermal boundary layers are formed. It can be seen that the high-momentum fluid entering the turn from the inflow passage impinges on the outer wall. As the flow turns into the second passage, the high-momentum flow again impinges on the outer wall. These flow impingements produced two distinct high heat transfer enhancement regions along the outer wall which will be discussed in detail in the next section. In the first passage, the velocity profile indicate a fully developed flow, at the beginning of the 180° sharp turn, the flow seems to be accelerated of near to the inner side and a flow separations occur almost at the same location of the thermal boundary layer. In the second pass, the flow is more accelerated in the outer side.

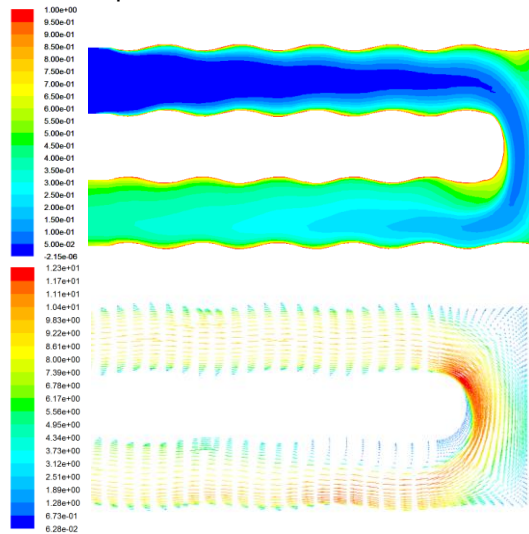
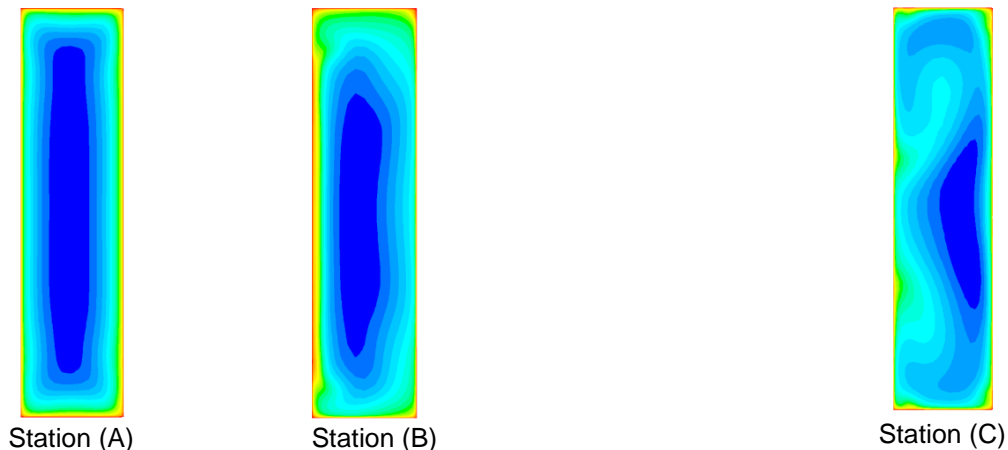


Fig.4: Dimensionless temperature contour and Velocity vectors in the middle plane of the rotating duct ( $Re = 10\,000$ ,  $R_0 = 0.14$ ,  $\Delta\rho/\rho = 0.13$ .)

Figure 5 shows the dimensionless temperature contour  $\theta$  and the vector field for  $Re = 10\,000$ ,  $R_0 = 0.14$ ,  $\Delta\rho/\rho = 0.13$  case at three axial Stations (A) ( $Z/D_h = 15.8$ ), (B) (midsection of the bend), and C ( $Z/D_h = 15.8$ ) as denoted in Fig. 1. It can be seen a perfect symmetry in directions of the temperature distribution at the section A and almost no secondary flow, the flow characteristics is identical to a simple flow through a straight channel. At the section B, exactly located at the middle of the 180° sharp turn, the distribution of the temperature is changed by decreasing its area and modifying its form. The cold air is concentrated in the center. More heat transfer occurs behind the outer surface. The anisotropy of the turbulent Reynolds stresses produced small secondary corner vortices in this section.



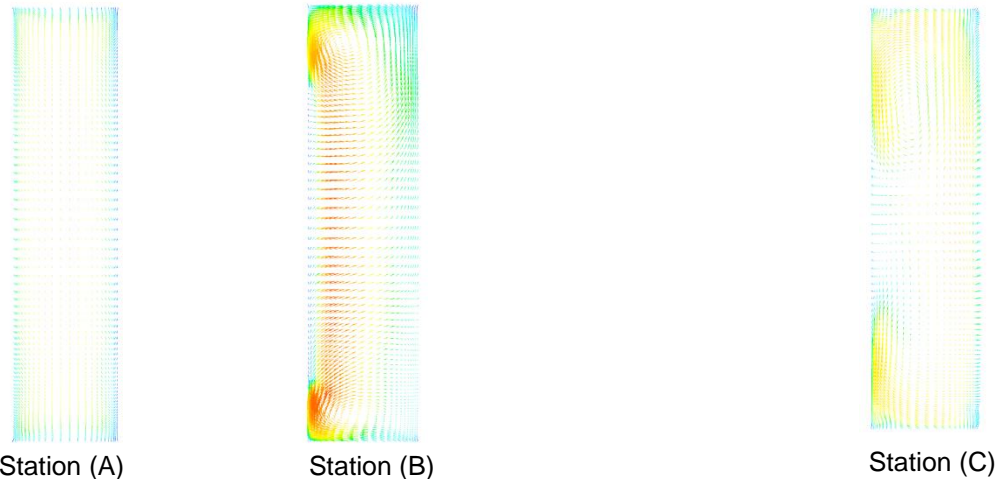


Fig.5: Dimensionless temperature contour and secondary flow vectors in the middle plane of the rotating duct ( $Re = 10\,000$ ,  $R_0 = 0.14$ ,  $\Delta\rho/\rho = 0.13$ ).

As the fluid flows through the 180° bend, the centrifugal forces arising from the curvature and the associated pressure gradients (low pressure at inner surface, high pressure at outer surface) produced a pair of counter-rotating vortices in the bend. These vortices are significantly stronger than those vortices observed in the first passage and are responsible for the transport of cool fluid from the core toward the outer surface. Before the bend, the cooler fluid is located in the core region. After the bend, however, the cooler fluid is pushed toward the outer surface by the centrifugal force induced by the streamline curvatures. This leads to steeper temperature gradients on the outer wall than on the inner wall after the bend as shown in Station (C) of Fig. 5. However, the nearly circular vortex pair is confined to the leading and trailing surfaces. Even though the secondary flow is very weak in the middle section of the channel, the additional pressure gradients induced by the counter-rotating vortices still apply over the entire channel cross-section. Consequently, the cooler fluid in the middle section of channel was pushed by the vortex-induced pressure gradients back towards the inner surface as seen in Station (B).

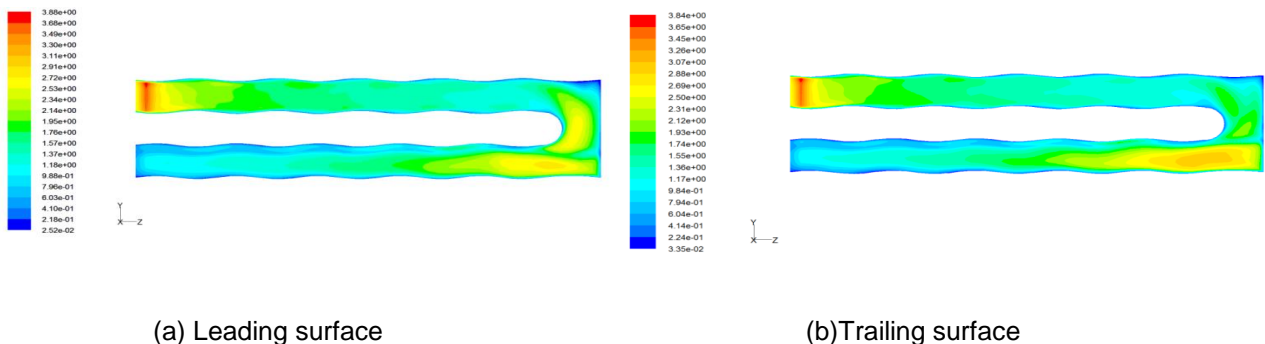


Fig.6: Nusselt number ratio contour on the heated section of the channel ( $Re = 10\,000$ ,  $R_0 = 0.14$ ,  $\Delta\rho/\rho = 0.13$ )

Figure 6 shows the  $Nu/Nu_0$  contour plots on the leading and trailing surfaces of the undulated channel with aspect ratio  $AR = 1:4$  for the rotating case ( $Re = 10\,000$ ,  $R_0 = 0.14$ ,  $\Delta\rho/\rho = 0.13$ ). In the first passage, the Nusselt number ratio is high near the inlet due to the thin thermal boundary layers. The heat transfer in the bend is high due to the secondary flows induced by the centrifugal forces and the associated pressure gradients. Downstream in the second passage, the heat transfer coefficient decreases and asymptotically approaches the fully developed value. In the first passage, the Nusselt number ratio on the trailing surface is higher than that on the leading surface. In contrast, in the second passage, the Nusselt number ratio on the leading surface is higher than that on the trailing surface. This agrees well with the analysis of the flow and temperature fields. On the leading surface, the Nusselt number ratio reaches minimum in the middle of the first passage and increases significantly in the bend. For the trailing surface, the Nusselt number ratio increases sharply in the

streamwise direction and reaches a maximum value in the bend region. In the second passage, the Nusselt number ratio decreases gradually along the duct.

Figure 7 presents the spanwise-averaged Nusselt number ratios for trailing and leading surfaces for the smooth channel without rotation predicted by both turbulence models:  $k-\omega$  SST and the second moment closure RSM compared to the experimental data obtained by Fu et al. (10) for the smooth rectangular channel to validate the numerical results in this study. The present simulation is carried out with the following operating conditions: ( $Re = 10\,000$ ,  $R_0 = 0.0$ ,  $\Delta\rho/\rho = 0.13$ ). For both trailing and leading surfaces, it is seen that the numerical predictions obtained by the  $k-\omega$  SST are in agreement with the experimental data in the first passage while the RSM predict well the heat transfer in the second pass. The discrepancy may be due to the fact that the flow conditions and thermal boundary conditions in the measurement are not completely consistent with the idealized condition in numerical prediction. Interesting to the sharp 180° turn and the second passage, the RSM seem to be better than the  $k-\omega$  SST model, it will be retained for all subsequent calculations.

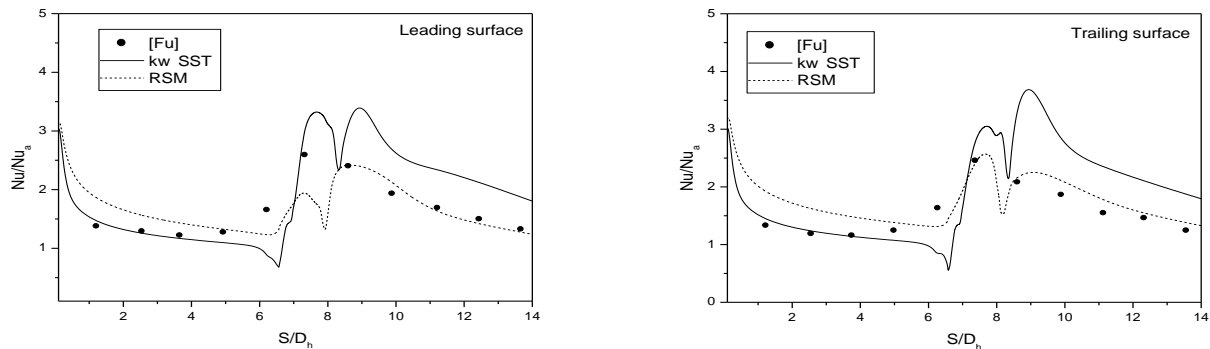


Fig.7: Comparison between calculated and measured Nusselt number ratios for non-rotating smooth rectangular channel ( $Re = 10\,000$ ,  $R_0 = 0.0$ ,  $\Delta\rho/\rho = 0.13$ ).

Figure 8 compare the heat transfer ratio on the trailing and the leading surfaces for both smooth and undulated rectangular channel under the same operating conditions ( $Re = 10\,000$ ,  $R_0 = 0.14$ ,  $\Delta\rho/\rho = 0.13$ ). It is clearly seen that the wavy feature with an undulation of 0.05 W of in amplitude created on the inner and the outer edges of the duct improve the heat transfer especially in the sharp 180° turn region by a net augmentation of the Nusselt number for both trailing and leading surfaces. As can be seen from this figure, the undulation effect increases the local Nusselt number and consequently the heat transfer. More heat transfer rate is transported towards the exit. Physically, the turbulent flow is more decelerated inside the channel by the presence of the undulation crests accumulating additional heat transfer and consequently a net increasing of the air temperature at the exit.

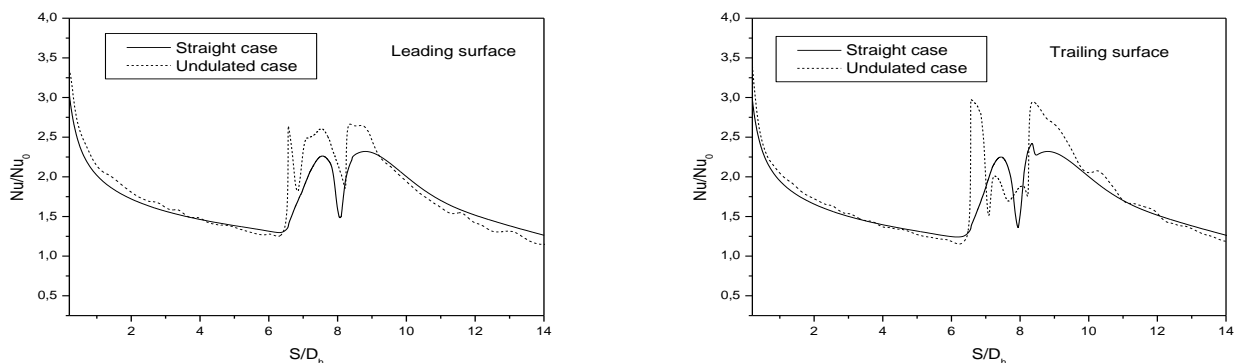


Fig. 8: Comparison of Nusselt number ratios for rotating smooth and undulated rectangular channel for the rotating case ( $Re = 10\,000$ ,  $R_0 = 0.14$ ,  $\Delta\rho/\rho = 0.13$ ).

Table 2 illustrates quantitatively the enhancement of the heat transfer ratio by comparing the Nusselt number on the trailing and the leading surfaces for both configurations; smooth and undulated. A net gain is obtained ranging from 4.8% on the trailing surface and practically the double value 9.6% on the

leading surface. Comparing the air temperature at the outlet of the second pass, a difference of 2.4 K is improved thanks to wavy walls.

	Smooth	Undulated
Nu Number Trailing surface	143.45	150.34
Nu Number Leading surface	140.61	154.11
Outlet Temperature (K)	316.8	319.2

Table 2. Comparison of the heat transfer characteristics between the smooth and undulated rectangular channel

Figure 9 depicts the local pressure coefficient distributions for the smooth rectangular channel case at the median plane and the sections A, B and C under the operating conditions ( $Re = 10\,000$ ,  $R_0 = 0.14$ ,  $\Delta p / \rho = 0.13$ ). It is seen that pressure gradient in the X direction is only present in the curved part, no significant difference is observed for the sections A and C contrary to the section B, where the pressure change considerably. The decrease of the pressure in the inner part of the curved bend tends to increase of the velocity field in this region. On the outer part of the sharp 180° turn, where the flow seems to be stopped, the pressure reaches its maximum.

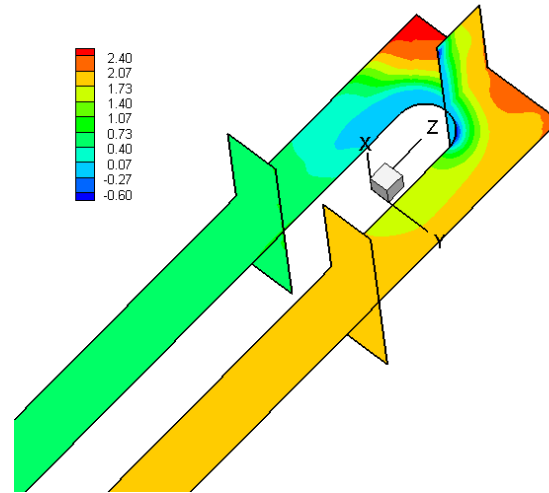


Fig. 9: Pressure coefficient on the median plane and the sections A, B and C ( $Re = 10\,000$ ,  $R_0 = 0.14$ ,  $\Delta p / \rho = 0.13$ ).

## 6 Summary

The three dimensional turbulent flow and convective heat transfer in two-pass smooth and wavy channels have been numerically investigated for an aspect ratio  $AR = 1:4$ . The numerical method was validated by comparing the results with the experimental data of Fu et al. (10). Using the commercial code ANSYS Fluent 6.3.26, it has been demonstrated that the second moment closure RSM model predict well the heat transfer comparing with  $k-\omega$  SST model especially in the 180° sharp turn. The presence of undulations on the leading and trailing surfaces induces an increase of the heat transfer namely in the sharp 180° turn region in comparison with the smooth duct due to deceleration of the fluid particles close to the crest of the undulations and consequently accumulating more heat transfer rate. Indeed the latter acts on the thermal boundary layer that is thickened or thinned along this wall. Consequently, an undulation feature is visible on the local Nusselt number distribution resulting in an increase of the heat transfer rate comparing to the smooth channel. Numerical tests comparing the smooth and the undulated configurations in the rotating two pass rectangular duct with an aspect ratio  $AR = 1:4$  ( $Re = 10\,000$ ,  $R_0 = 0.14$ ,  $\Delta p / \rho = 0.13$ ) show that the fluid at the outlet of the wavy duct is more heated by 2.4 K compared to the smooth one.



## 7 Literature

- [1] Wagner, J. H, Johnson, B. V., Han, J. C., , "Heat transfer in rotating passages with smooth walls and radial outward flow", *Journal of Turbomachinery*, 113(1), 1991, pp. 42-51.
- [2] Guoguang, S., Hamn-Ching, C., Je- Chin, H., "Computation of flow and heat transfer in rotating two-pass rectangular channels (AR = 1:1, 1:2, and 1:4) with smooth walls by a Reynolds stress turbulence model", *Int. J. Heat Mass Transfer* (47), 2004, pp. 5665–5683.
- [3] Johnson, B. V., Wagner, J. H, Steuber, G. D., "Heat transfer in rotating serpentine passages with trips skewed to the flow", *Journal of Turbomachinery* 116(1), , 1994,pp.113-123.
- [4] D.M. McGrath, D.G.N. Tse, 1995, "A combined experimental/ computational study of flow in turbine blade cooling passage. Part 2.Numerical simulations", Paper 95-GT-149, ASME.
- [5] Al-Qahtani, M. S., Jang. Y. J., Chen, H. C., "Prediction of flow and heat transfer in rotating two-pass rectangular channels with 45-deg rib turbulators", *Journal of Turbomachinery*124(2), 2002,pp.242-250.
- [6] Dutta, S., Andrews, M. J., Han J. C., "Prediction of turbulent heat transfer in rotating smooth square ducts", *International Journal of Heat and Mass Transfer* 39(12),1996, pp. 2505-2514.
- [7] Chen, H. C., Jang, Y. J., Han, J. C., "Near-wall second- moment closure for rotating multi-pass cooling channels", *Journal of Thermophysics and Heat Transfer* 14 (2), 2000,pp. 201-209.
- [8] E. Lee, L.M. Wright, J.C. Han, "Heat transfer in rotating rectangular channels (AR = 4:1) with V-shaped and angled rib turbulators with and without gaps", ASME Paper Number GT-2003-38900.
- [9] Iacovides, H., Launder, B.E., Li, H.Y., "The computation of flow development through stationary and rotating U-ducts of strong curvature", *Int. J. Heat Fluid Flow* 17 (1), 1996,pp. 22–33.
- [10] Fu, W.L., Wright L., Han, J. C., "Heat transfer in two-pass rotating rectangular channels (AR = 1:2 and AR = 1:4) with 45° angled rib turbulators, ASME Paper GT 2004- 53261.
- [11] F.R.Menter M.Kuntz R.Langtry Ten years of industrial Experience with the SST Turbulence Model. Department Ansys CFX-83714 Otterfing Germany 2003

## 8 Nomenclature

$AR$	channel aspect ratio
$D_h$	hydraulic diameter
$H$	heat transfer coefficient
$K$	thermal conductivity of coolant
$L$	total length of the channel
$L_1$	unheated smooth starting section of the channel
$L_2$	heated section of the channel
$Nu$	local Nusselt number, $h D_r/k$
$Nu_0$	Nusselt number in fully-developed turbulent non-rotating tube ( $Nu_0 = 0.023 Re^{0.8} Pr^{0.4}$ )
$Pr$	Prandtl number, $Pr = \nu/a$
$Re$	Reynolds number, $Re = \rho W_b D_h / \mu$
$R_0$	rotation number, $R_0 = \Omega D_h / W_b$
$R_r$	radius from axis of rotation
$S$	streamwise distance
$T$	local coolant temperature
$W_b$	bulk velocity in streamwise direction